

Multicomponent heat and mass transfer for flow over a droplet

P. L. C. LAGE† and R. H. RANGEL

Department of Mechanical and Aerospace Engineering, University of California,
Irvine, CA 92717, U.S.A.

and

C. M. HACKENBERG

Department of Chemical Engineering—COPPE, Federal University of Rio de Janeiro,
21945 Rio de Janeiro, Brazil

(Received 7 April 1992 and in final form 9 October 1992)

Abstract—The solution of the constant-property boundary-layer equations for momentum, mass, and energy transport, including blowing, surface tangential displacement, and the interdiffusion term, in the flow over a vaporizing sphere is obtained by series solution retaining the first three terms. The results of a large number of calculations are presented in the form of ratios of Nusselt and Sherwood numbers with and without phase change for mono and bicomponent droplets. These calculations span a large range of the mass and heat transfer numbers, which are used to correlate the results. A global interdiffusion parameter is defined and also used to correlate the Nusselt number ratio. High order correlations are also presented. The validity of the correlations for nonzero surface tangential velocity is evaluated through sensibility analysis. The results show that one can use the obtained correlations for the blowing effect for a general surface velocity condition.

INTRODUCTION

MASS AND energy exchanges between a dispersed phase and a continuous convective flow occur frequently in several practical situations. Direct heat transfer vaporization, liquid–liquid extraction, spray drying and spray combustion are common examples. In the analysis of such complex phenomena, it is common to study the behavior of only one particle of the dispersed phase which is assumed to be spherical. Particle interactions are usually incorporated as correction factors. When heat and mass transfer occur simultaneously, the coupling of mechanisms becomes possible. The flow caused by phase change (Stefan flow) modifies the flow conditions, increasing the characteristic lengths for heat and mass transfer with a consequent reduction in their rates. Moreover, the interdiffusion of species with different partial molar enthalpies generates an extra term in the energy conservation equation. The existence of coupled boundary conditions at the sphere surface contributes to the complexity of the phenomenon.

In spray applications, the phenomena of interest occur in the low to moderate Reynolds number regime. Furthermore, it is desirable to have a simple yet accurate droplet submodel to be used in spray calculations. Accordingly, several simplifying hypotheses have been proposed and evaluated in the past.

For stagnant environments, Hubbard *et al.* [1] verified that the quasi-steadiness of gas-transport processes is justifiable for low to moderate pressures (up to 10 atm). They also verified that a reference state can be used to calculate the gas properties, and they recommended the '1/3 rule'. The use of quasi-steady correlations for drag, Nusselt, and Sherwood number for the transient vaporization of a heptane droplet in its own vapor and in air has been investigated by Renksizbulut and Haywood [2], Haywood *et al.* [3] and Renksizbulut *et al.* [4] through comparison with fully numerical results. They have found that such correlations can account for variable properties effects and droplet transient heating provided convenient film conditions and an effective latent heat are defined. However, Bussmann and Renksizbulut [5] verified that the drag coefficient is not well predicted by the existing steady-state correlation for very volatile fuel droplets.

These quasi-steady correlations for the Nusselt and Sherwood numbers can be obtained through experiments [6, 7] or by theoretical calculations through either numerical solution of the conservation equations [4, 8], or boundary-layer approximation [9]. The last approach consists in matching the boundary-layer solution and the analytical solution for the stagnant droplet case. This matching procedure is an extension of the film theory that incorporates the thickening of the film due to the Stefan flow, and is called extended film theory [10]. It reduces to the classical film theory [11] as the transfer numbers tend to zero and con-

† On leave from Department of Chemical Engineering—COPPE/UFRJ, Brazil.

NOMENCLATURE

B_i	mass transfer number	y	normal coordinate
B_{m_i}	modified mass transfer number for component i , $(Y_i - Y_{i_s}) / \left(1 - \sum_{j=1}^N Y_{j_s}\right)$	Y	mass fraction.
B_1	heat transfer number	Greek symbols	
B_T	heat transfer number based on mixture specific heat	γ_i	ratio between the partial specific heat of the component i in the mixture and the specific heat of the mixture, C_{p_i}/C_p
C_p	specific heat at constant pressure	Γ_i	interdiffusion heat transfer parameter, $(\gamma_i - \gamma_g Sc_i/Sc_g)(Y_i - Y_{i_s})$
f	function in ψ series expansion	δ	fraction of the ideal flow tangential velocity which is imposed to the sphere surface
h	function in Θ series expansion	Δ	global interdiffusion parameter
H	effective latent heat, Q_T/\dot{m}	ε	fraction rate of mass changing state
k	thermal conductivity	ζ	dimensionless surface-axis of symmetry distance, $r/R = \sin \zeta$
\dot{m}	rate of mass changing phase	η	dimensionless normal coordinate, y/R
M	dimensionless rate of mass changing phase, $\dot{m}/(2\pi R^2 \rho u_x)$	$\bar{\eta}$	$\sqrt{(3Re)\eta}$
N	number of components in the liquid sphere	Θ	dimensionless temperature, $(T - T_s)/(T_x - T_s)$
Nu	Nusselt number	ν	kinematic viscosity
p	function in Π series expansion	ξ	dimensionless tangential coordinate, x/R
Pe	Peclet number, $Re Pr$	Π	dimensionless mass fraction, $(Y - Y_s)/(Y_x - Y_s)$
Pe_m	mass transfer Peclet number, $Re Sc$	ρ	density
Pr	Prandtl number	ψ	stream function.
Q_T	heat transfer rate to the sphere	Subscripts	
\mathcal{Q}_T	dimensionless heat transfer rate to the sphere, $Q_T/(\pi Rk(T_x - T_s))$	D	diameter based
r	surface-axis of symmetry distance	e	ideal flow
R	sphere radius	g	gas phase
Re	Reynolds number, $u_x R/\nu$	i	component i or function i
Sc	Schmidt number	s	sphere surface
Sh	Sherwood number	∞	free stream.
T	temperature	Superscripts	
u	tangential velocity	i	component i
u_c	ideal flow tangential velocity	0	without phase change.
U	dimensionless tangential velocity, u/u_x , or the coefficients in its series expansion		
U_c	ideal flow dimensionless velocity, $u_c/u_x = 1.5 \sin \zeta$		
v	normal velocity		
V	dimensionless normal velocity, v/u_x		
x	tangential coordinate		

veniently separates the Nusselt and Sherwood numbers into stagnant and convective contributions in the form:

$$Nu_D = \left[2 + \frac{Nu_D^0 - 2}{\left(\frac{Nu_D^0}{Nu_{D,C}} \right) \frac{\ln(1+B_i)}{B_i}} \right] \frac{\ln(1+B_i)}{B_i} \quad (1)$$

where $(Nu_D^0/Nu_{D,C})$ is the ratio of Nusselt numbers without and with vaporization for the large Reynolds number approximation. A similar equation holds for the Sherwood number. The reduction in the Nusselt and Sherwood numbers due to blowing, for the large

Reynolds number range, has been represented by the factor $(1+B)^{-0.7}$, where B is either B_1 or B_i and $B_i \leq 20$. These results have been obtained for flow over wedges and used in the sphere problem under the hypothesis of independence of geometry. The interdiffusion term was neglected in the energy conservation equation.

The Nusselt number correlation obtained by Renksizbulut and Yuen [7] and the Sherwood correlation given by Renksizbulut *et al.* [4] also present a $(1+B)^{-0.7}$ factor to account for the reduction of the transport processes due to blowing. The Nusselt number correlation is based on experiments with

monocomponent droplet where $B_i < 2.8$ and has been successfully used to predict the Nusselt number history in the transient vaporization of heptane droplets by Renksizbulut and Haywood [2] and Haywood *et al.* [3]. However, they did not report the B_i number range obtained in their numerical simulations. The interdiffusion term was accounted for in the energy equation but no attempt has been made to verify its direct influence on the Nusselt number. The above-cited numerical simulations have been used by Renksizbulut *et al.* [4] to derive their Sherwood number correlation, which compared well with the data of Downing [12] and Renksizbulut [13]. The B_i number range obtained in the simulations was not reported, but it can be inferred from their Fig. 1 that $B_i < 2.2$. They compared the correlation predictions to the Sherwood number history numerically obtained for the vaporization of a decane-hexadecane mixture. Although the agreement was fairly good, the B_i number range was not reported. Bussmann and Renksizbulut [5] numerically simulated the vaporization of a very volatile liquid droplet and compared the obtained Nusselt and Sherwood numbers to those given by the correlations of Renksizbulut and Yuen [7] and Renksizbulut *et al.* [4]. The agreement was fairly good. For this case B_T was as large as 61 and B_i was around 10.

In the works cited above, the effect of blowing has only been correlated for low transfer numbers. However, for multicomponent droplets, the mass transfer number is defined in terms of the fractional vaporization rate and can indeed assume very large values (up to 100). Besides, the heat transfer number can be quite large for a very volatile fuel droplet. The results so far show that the reduction in the Nusselt and Sherwood numbers due to blowing can be represented by a $(1+B)^{-0.7}$ factor, with no dependence on the Reynolds or Prandtl (Schmidt) numbers. However, even though the interdiffusion term in the energy conservation equation is considered in deriving the film theory, its direct effect in the Nusselt number has not been analyzed yet for convective fields. Another point that still needs further investigation is the influence of surface velocity on the Nusselt and Sherwood numbers. This velocity can be indeed quite appreciable: Renksizbulut and Haywood [2] and Haywood *et al.* [3] obtained maximum surface tangential velocities as large as 24% of the free stream velocity. However, they did not carry out a systematic study of the effect of surface velocity in the correlations used to predict Nusselt and Sherwood number behavior. It should be pointed out that most of the experiments carried out on droplet vaporization have been performed with porous spheres or suspended droplets where internal circulation is partially or completely eliminated.

Thus there are still some restrictions in the applicability of the existing correlations for Nusselt and Sherwood numbers, and further investigation is necessary. In order to eliminate some of the above-

cited restrictions, the present work carries out a parametric analysis of the solution of the momentum, energy and mass boundary layer equations for flow over a sphere. The framework of the extended film theory is adopted here, and the ratios of the Nusselt and Sherwood numbers with and without phase change are determined, under the boundary-layer approximation, and correlated with the transfer numbers. The boundary-layer analysis does lead to an underestimation of the Nusselt and Sherwood numbers, because it cannot account for the wake region. However, this error has been estimated to be around 15% [3, 14], which should not appreciably affect the functional form of the blowing correction. The basic goals are to expand the range of transfer numbers in the blowing correction, to determine the direct effect of the interdiffusion term on the heat transfer, and to evaluate the effect of tangential surface velocity on correlations derived for no tangential velocity.

ANALYSIS

Some basic assumptions are used in applying the steady laminar boundary layer theory to the heat and mass transport phenomena in a fluid flowing over a sphere. These assumptions are:

- (1) The Reynolds number is high enough so that the boundary layer approximation is applicable and the gravitational forces are negligible;
- (2) Curvature effects are negligible;
- (3) The Stefan flow is not enough to blow out the boundary layer;
- (4) The free stream fluid is not soluble in the liquid sphere;
- (5) Mass diffusion is considered to be given by Fick's law;
- (6) The physical properties of the fluid are constant;
- (7) Viscous dissipation is negligible and the pressure variation effect in the energy transport does not need to be considered (small Eckert number).

In addition, it is at first assumed that the surface tangential velocity is negligible. The effect of this assumption on the heat and mass transfer phenomena will be then examined by considering the surface tangential velocity to be a fraction of the ideal flow velocity over a sphere. Hypotheses (1) and (2) are reasonably met for the Reynolds number range used to obtain the asymptotic behavior of the Nusselt and Sherwood numbers for high Reynolds numbers ($100 \leq Re_D \leq 1000$). Hypothesis (3) above is met by requiring that the boundary layer thickness for the case with phase change does not surpass the thickness for the case without phase change in more than 20%. Hypothesis (5) is only to simplify the analysis and hypothesis (6) is in agreement with the utilization of film conditions for the fluid in the boundary layer. Hypothesis (7) is non-restrictive for the Reynolds number range analyzed. The boundary conditions for

heat and mass transfer at the sphere surface are constant temperature and concentration. This agrees with any uniform-surface temperature liquid phase model where the composition at the surface is calculated through phase-equilibrium at the given surface temperature.

Using the above assumptions, the steady laminar boundary layer equations for mass, momentum and energy conservation can be written in dimensionless form as

$$\frac{1}{\zeta} \frac{\partial}{\partial \zeta} (\zeta U) + \frac{\partial V}{\partial \eta} = 0 \tag{2}$$

$$U \frac{\partial U}{\partial \zeta} + V \frac{\partial U}{\partial \eta} = U_c \frac{dU_c}{d\zeta} + \frac{1}{Re} \frac{\partial^2 U}{\partial \eta^2} \tag{3}$$

$$U \frac{\partial \Pi_i}{\partial \zeta} + V \frac{\partial \Pi_i}{\partial \eta} = \frac{1}{Pe_m} \frac{\partial^2 \Pi_i}{\partial \eta^2}, \quad i = 1, \dots, N \tag{4}$$

$$U \frac{\partial \Theta}{\partial \zeta} + V \frac{\partial \Theta}{\partial \eta} = \frac{1}{Pe} \frac{\partial^2 \Theta}{\partial \eta^2} + \Theta \sum_{i=1}^N \frac{\Gamma_i}{Pe_m} \frac{\partial^2 \Pi_i}{\partial \eta^2} \tag{5}$$

The boundary conditions are

$$\eta = 0, \quad U = \delta U_c(\zeta), \quad \Pi_i = 0, \quad \Theta = 0,$$

$$V = \sum_{i=1}^N \frac{B_{m_i}}{Pe_m} \frac{\partial \Pi_i}{\partial \eta} \tag{6}$$

$$\eta \rightarrow \infty, \quad U = U_c(\zeta), \quad \Pi_i = 1, \quad \Theta = 1. \tag{7}$$

A stream function can be defined to satisfy the continuity equation (equation 2) as

$$U = \frac{\partial \psi}{\partial \eta}, \quad V = -\frac{1}{\zeta} \frac{\partial}{\partial \zeta} (\zeta \psi). \tag{8}$$

Then ψ , U_c , ζ can be expanded in series of odd powers of ζ (odd functions) and Π_i and Θ in series of even powers of ζ (even functions):

$$\zeta(\zeta) = \sum_{j=0}^{\infty} \zeta_{2j+1} \zeta^{2j+1} \tag{9}$$

$$U_c(\zeta) = \sum_{j=0}^{\infty} U_{2j+1} \zeta^{2j+1} \tag{10}$$

$$\psi(\zeta, \bar{\eta}) = \frac{1}{\sqrt{(3 Re)}} \sum_{j=0}^{\infty} U_{2j+1} \zeta^{2j+1} f_{2j+1}(\bar{\eta}) \tag{11}$$

$$\Pi_i(\zeta, \bar{\eta}) = \sum_{j=0}^{\infty} \zeta^{2j} p_{2j}^i(\bar{\eta}), \quad i = 1, \dots, N \tag{12}$$

$$\Theta(\zeta, \bar{\eta}) = \sum_{j=0}^{\infty} \zeta^{2j} h_{2j}(\bar{\eta}) \tag{13}$$

where $\bar{\eta} = \sqrt{(3 Re)} \eta$ is a scaled normal coordinate due to the small thickness of the boundary layer.

Using equations (8)–(13) in equations (2)–(5), and after some algebraic manipulation, the ordinary differential equation systems for the first three terms in each series are given by

$$2f_1''' + 2f_1 f_1'' + 1 - f_1'^2 = 0 \tag{14}$$

$$\frac{1}{Sc_i} p_0^{i''} + f_1 p_0^{i'} = 0, \quad i = 1, \dots, N \tag{15}$$

$$\frac{1}{Pr} h_0'' + f_1 h_0' + h_0 \sum_{i=1}^N \frac{\Gamma_i}{Sc_i} p_0^{i''} = 0 \tag{16}$$

$$f_3''' + f_1 f_3'' - 2f_1' f_3' + 2f_1'' f_3 + f_1 f_1'' + 2 = 0 \tag{17}$$

$$\frac{1}{Sc_i} p_2^{i''} + f_1 p_2^{i'} - f_1' p_2^i - \frac{1}{6} (f_1 + 2f_3) p_0^{i'} = 0, \tag{18}$$

$$i = 1, \dots, N$$

$$\frac{1}{Pr} h_2'' + f_1 h_2' + \left(\sum_{i=1}^N \frac{\Gamma_i}{Sc_i} p_0^{i''} - f_1' \right) h_2 + \left[h_0 \sum_{i=1}^N \frac{\Gamma_i}{Sc_i} p_2^{i''} - \frac{1}{6} (f_1 + 2f_3) h_0' \right] = 0 \tag{19}$$

$$f_5''' + f_1 f_5'' - 3f_1' f_5' + 3f_1'' f_5 - 5f_3'^2 + \frac{10}{3} (2f_3 + f_1) f_3'' + \left(\frac{10}{3} f_3 - \frac{4}{3} f_1 \right) f_1'' + 8 = 0 \tag{20}$$

$$\frac{1}{Sc_i} p_4^{i''} + f_1 p_4^{i'} - 2f_1' p_4^i + \left(\frac{4}{30} f_3 + \frac{1}{36} f_3 - \frac{1}{90} f_1 \right) p_0^{i'} - \frac{1}{6} (2f_3 + f_1) p_2^{i'} + \frac{1}{6} f_3' p_2^i = 0, \quad i = 1, \dots, N \tag{21}$$

$$\frac{1}{Pr} h_4'' + f_1 h_4' + \left(\sum_{i=1}^N \frac{\Gamma_i}{Sc_i} p_0^{i''} - 2f_1' \right) h_4 + \left(\sum_{i=1}^N \frac{\Gamma_i}{Sc_i} p_4^{i''} \right) h_0 + \left(\sum_{i=1}^N \frac{\Gamma_i}{Sc_i} p_2^{i''} + \frac{1}{6} f_3'' \right) h_2 + \left(\frac{4}{30} f_3 + \frac{1}{36} f_3 - \frac{1}{90} f_1 \right) h_0' - \frac{1}{6} (2f_3 + f_1) h_2' = 0 \tag{22}$$

where the primes represent differentiation with respect to $\bar{\eta}$. The boundary conditions become

$$\bar{\eta} = 0, \quad f_{2j+1} = \delta, \quad p_{2j}^i = 0, \quad h_{2j} = 0, \tag{23}$$

$$i = 1, \dots, N, \quad j = 0, 1, 2.$$

$$f_1 = - \sum_{i=1}^N \frac{B_{m_i}}{Sc_i} p_0^{i'}$$

$$f_3 = \sum_{i=1}^N \frac{B_{m_i}}{Sc_i} (3p_2^{i'} + \frac{1}{2} p_0^{i'})$$

$$f_5 = - \sum_{i=1}^N \frac{B_{m_i}}{Sc_i} \left(\frac{1}{36} p_0^{i'} + \frac{1}{10} p_2^{i'} + p_4^{i'} \right)$$

$$\bar{\eta} \rightarrow \infty, \quad f_{2j+1} = 1, \quad j = 0, 1, 2, \quad p_0^i = 1, \quad h_0 = 1, \tag{24}$$

$$p_{2j}^i = 0, \quad h_{2j} = 0, \quad j = 1, 2, \quad i = 1, \dots, N.$$

It is interesting to notice that the interdiffusion term in the energy equation is present even in the differential equation for the zeroth-order component in the temperature expansion, h_0 .

The separation point of the flow is determined using the condition of zero tangential stress with the first two terms in the velocity series expansion (the three term approximation is unable to determine a real value for the separation point). Although this is a crude approximation for the separation point, it does not significantly affect global quantities for the heat and mass transfer processes. Since there are large gradients of temperature and concentration only near

the front stagnation point, the contributions for global quantities of the wake region and regions near the separation point are usually small. Accordingly, the error in neglecting the wake region in the heat and mass transfer processes has been estimated by Prakash and Sirignano [14] to be less than 15% and Haywood *et al.* [3] obtained values under 10% in their numerical calculations. Since this error is present in both the vaporizing and non-vaporizing cases, it is believed that it will not affect the functional form of the blowing effect correction.

Once the separation point, ξ_s , is known, the global quantities are determined through integration. The most important global quantities are the dimensionless rate of phase change and the total heat transfer to the sphere which are given by

$$M_i = \int_0^{\xi_s} \zeta \sum_{j=1}^N \frac{B_m Y_k - \delta_{ij}(Y_i - Y_k)}{Pe_{m_j}} \left(\frac{\partial \Pi_j}{\partial \eta} \right)_{\eta=0} d\xi \quad (25)$$

$$\mathcal{Q}_T = 2 \int_0^{\xi_s} \zeta \left(\frac{\partial \Theta}{\partial \eta} \right)_{\eta=0} d\xi \quad (26)$$

where δ_{ij} is the Kronecker delta. These quantities allow one to define the mass and heat transfer numbers

$$B_i = \frac{Y_k - Y_i}{\varepsilon_i - Y_k} \quad (27)$$

$$B_t = \frac{\sum_{i=1}^N \varepsilon_i C_p (T_x - T_s)}{H} = \frac{M Pe_D}{\mathcal{Q}_T} \sum_{i=1}^N \varepsilon_i \gamma_i \quad (28)$$

where H is the effective latent heat and

$$M = \sum_{i=1}^N M_i, \quad \varepsilon_i = \frac{M_i}{M}. \quad (29)$$

The mean Nusselt and Sherwood number can be determined by integration of the local Nusselt and Sherwood numbers and division by the total sphere surface area, which results in

$$Nu_D = \int_0^{\xi_s} \zeta \left(\frac{\partial \Theta}{\partial \eta} \right)_{\eta=0} d\xi \quad (30)$$

$$Sh_{D,i} = \int_0^{\xi_s} \zeta \left(\frac{\partial \Pi_i}{\partial \eta} \right)_{\eta=0} d\xi. \quad (31)$$

There are another two dimensionless numbers of interest, the heat transfer number based on the mixture specific heat, B_T , and the global interdiffusion parameter, Δ

$$B_T = \frac{B_t}{\sum_{i=1}^N \varepsilon_i \gamma_i} = \frac{C_p (T_x - T_s)}{H} \quad (32)$$

$$\Delta = \prod_{i=1}^N \left(1 + \frac{\Gamma_i}{Sc_i} \right). \quad (33)$$

NUMERICAL PROCEDURE

The basic problem consists of solving the two-point boundary value problem given by equations (14)–(24). This system of nonlinear ordinary differential equations is transformed in a system of first order nonlinear ordinary differential equations which is then solved by the routine DBVFPD of the IMSL library (version 10) with a required tolerance of 0.1% in all variables and their derivatives. The boundary condition at $\eta \rightarrow \infty$ is assumed at a point far enough from the sphere surface. It has been found that $\eta = 0.8$ provides converged results. The DBVFPD routine performs the solution of the system of first order differential equations using the variable order, variable step size finite-difference method with deferred correction proposed by Pereyra [15]. The system Jacobian has been calculated analytically and used with BVFPD routine. As a check the routine itself is allowed to calculate the Jacobian by finite-differences, and the same results were obtained. Once f_{2j+1} , h_{2j} , p'_{2j} and their derivatives are known, all the relevant quantities are determined analytically.

RESULTS AND DISCUSSION

Firstly, the Nusselt number for a sphere without phase change has been determined for several Reynolds and Prandtl numbers and assumed surface velocities. The contribution of the third term in the series expansions to the Nusselt number value proved to be quite small, having a maximum value of 0.65%. The correlations obtained and related information are summarized in Table 1. All these correlations give the expected Nu_D^0 dependence with the square root of Re_D . Moreover, the Nu_D^0 correlation for no surface velocity is in good agreement with the convective part of the Ranz and Marshall [6] and Renksizbulut and Yuen [7] (without vaporization) correlations. The discrepancies in the multiplying constant and Pr exponent correspond to the expected underestimation of the Nusselt number, being below 15% (for $Pr \leq 20$). This gives good confidence in the series solution approximation developed above. It should be pointed out that the correlations obtained from experiments with droplets could have some effect on tangential surface velocity. For instance, the multiplying constants of previous correlations [6, 7] are within the range of values obtained when a tangential velocity is imposed at the surface. Using the heat–mass transfer analogy, the Sherwood number in the limit of no mass transfer has the same functional form obtained for the Nusselt number, that is

$$Nu_D^0(Re_D, Pr) = Sh_D^0(Re_D, Sc). \quad (34)$$

A large number of simulations were performed for mono and bicomponent liquid spheres at different values of the governing parameters in equations (2)–(5), spanning the ranges:

$$100 \leq Re_D \leq 1000,$$

Table 1. Calculations for cases without phase change. The correlation is $Nu_D^0 = a Re_D^b Pr^c$. Ranges: $50 \leq Re_D \leq 1000$ and $0.5 \leq Pr \leq 20$. Maximum relative error of correlation: 0.6%

% of ideal flow velocity assumed at the sphere surface	Number of calculations	Parameters		
		<i>a</i>	<i>b</i>	<i>c</i>
0	81	0.5314	0.5000	0.3588
10	81	0.5679	0.5000	0.3904
20	81	0.6023	0.5000	0.4143
30	81	0.6350	0.5000	0.4331

$$0.5 \leq Pr, Sc \leq 20,$$

$$\gamma_i - \gamma_g Sc_i / Sc_g \leq 5,$$

$$0.1 \leq B_m \leq 20.$$

After solving the two-point boundary layer problem, the results are analyzed and they are rejected if the contribution of the third term in series solution to the Nusselt and Sherwood numbers is larger than 5% or the thickness of the boundary layer in the separation point corresponds to an increase above 20% over the thickness for the case without phase change. These conditions are imposed to restrict the analysis to the cases where the boundary layer approximation should be valid. The valid calculations summed up to more than 1100 for a monocomponent and more than 1400 for a bicomponent liquid sphere. These result in about 2600 data points for the ratio Nu_D / Nu_D^0 and about 4000 data points for the ratio Sh_D / Sh_D^0 . All these data points cover the following range of dimensionless numbers:

$$0 < B_i < 90,$$

$$0 < B_T < 175$$

$$1 < \Delta < 12.5.$$

The traditional correlation of the ratio of the Nusselt numbers with and without phase change is given by

$$\frac{Nu_D}{Nu_D^0} = (1 + B_i)^a \tag{35}$$

and a similar correlation exists for Sh_D and B_i . These correlations are presented in Figs. 1 and 2, for the Nusselt and Sherwood numbers, respectively. The exponent a is found by regression to be -0.711 for heat transfer and -0.689 for mass transfer. Both exponents are very close to the value -0.7 given by previous correlations [4, 9, 7], some of which based on experimental data. The maximum and mean errors for the correlations are, respectively, 36% and 6% for the Nusselt number ratio and 20% and 3.5% for the Sherwood number ratio. Although a single coefficient can fairly describe both phenomena, there is a large scatter in the Nusselt number ratio and the two sets of data points undoubtedly present curvatures. These trends have not been noted in the previous works because those were restricted to small transfer

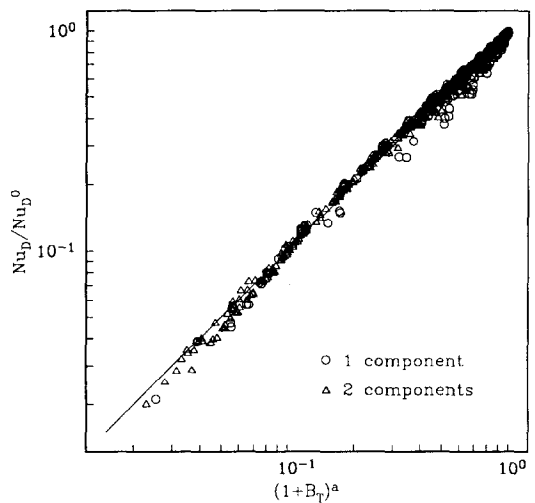


FIG. 1. Effect of mass transfer on Nusselt number—classical correlation ($a = -0.711$).

numbers. The large data scatter was expected due to the attempt of representing the blowing corrections by a prescribed functional form in terms of combined parameters (the transfer numbers).

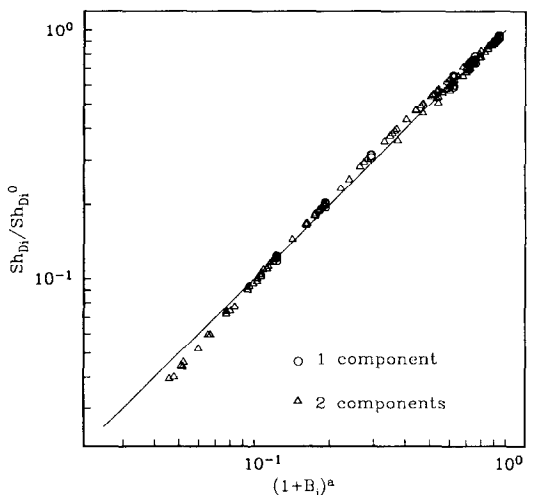


FIG. 2. Effect of mass transfer on Sherwood number—classical correlation ($a = -0.689$).

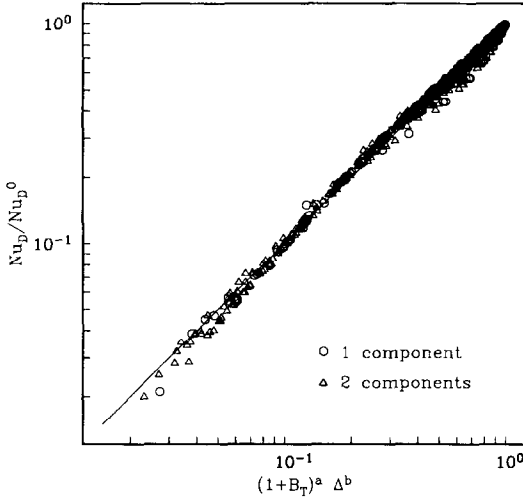


FIG. 3. Nusselt number correlation including the global interdiffusion parameter, Δ ($a = -0.690$ and $b = -0.178$).

The large scattering observed in the Nusselt number ratio is partially due to the effect of interdiffusion. An equation of the form

$$\frac{Nu_D}{Nu_D^0} = (1 + B_T)^a \Delta^b \quad (36)$$

has been used to correlate the data attempting to incorporate the effect of interdiffusion and the following parameters were obtained: $a = -0.690$ and $b = -0.178$, with a maximum error of 30% and a mean error below 3%. This correlation and the data points are shown in Fig. 3. Besides the improvement in the correlation with a decrease in the data scattering, it is remarkable that the exponent of $(1 + B_T)$ has not been much altered and that its value is basically the same obtained for the exponent of $(1 + B_i)$ in the Sherwood correlation. Such agreement corroborates the validity of Δ as a dimensionless number to incorporate the effect of interdiffusion in the analysis. However, there is still curvature in the data points in the log-log representation. It should be noticed that the effect of the interdiffusion term vanishes for no vaporization and increases as the Sc_i number decreases, as one would expect from physical considerations.

As an attempt to better represent the data, a second order polynomial in the logarithm of $(1 + B_T)$ for heat transfer and of $(1 + B_i)$ for mass transfer has been used. Keeping the global interdiffusion parameter, Δ , we propose the following correlations

$$\frac{Nu_D}{Nu_D^0} = (1 + B_T)^a \Delta^b \exp[c \ln^2(1 + B_T)] \quad (37)$$

where $a = -0.651$, $b = -0.192$ and $c = -0.0126$, with maximum error of 24% and mean error below 3%, and

$$\frac{Sh_{D_i}}{Sh_{D_i}^0} = (1 + B_i)^a \exp[b \ln^2(1 + B_i)] \quad (38)$$

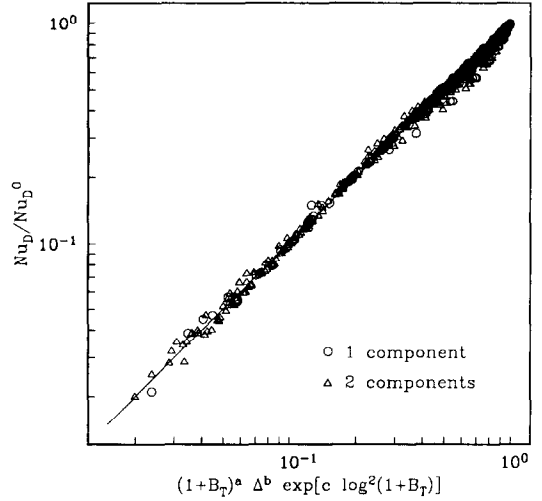


FIG. 4. High order correlation for the effect of mass transfer on the Nusselt number, including the effect of interdiffusion in the energy conservation equation ($a = -0.651$, $b = -0.192$ and $c = -0.0126$).

where $a = -0.619$, $b = -0.0230$, with a maximum error of 11% and a mean error of 2%. These two correlations, as well as the data points used to generate them, as presented in Figs. 4 and 5, for the Nusselt and Sherwood number ratio, respectively. It can be seen that the data points are in very good agreement with the correlated straight lines. The improvement is really remarkable for the Sherwood number ratio correlation, being only marginal for the Nusselt number ratio correlation. As obtained in previous works, no dependence on Re_D , Pr or Sc has been found in the correction for mass transfer.

The effect of existence of tangential surface velocity is verified by assuming that it is given by a fraction of the velocity of the ideal flow past a sphere. From

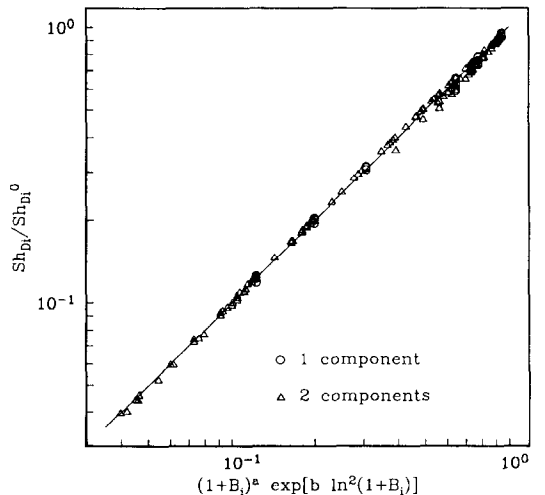


FIG. 5. High order correlation for the effect of mass transfer on the Sherwood number ($a = -0.619$ and $b = -0.0230$).

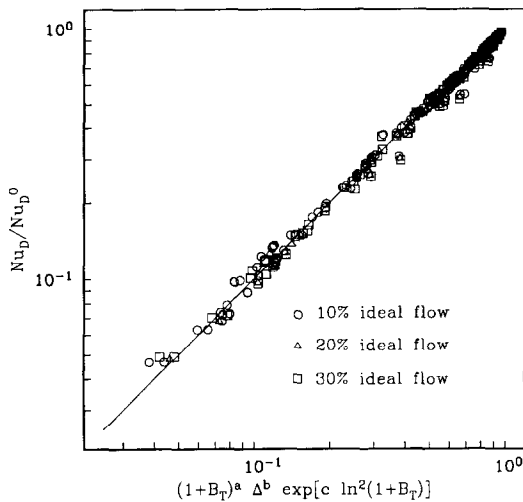


FIG. 6. Effect of tangential surface velocity on Nusselt number.

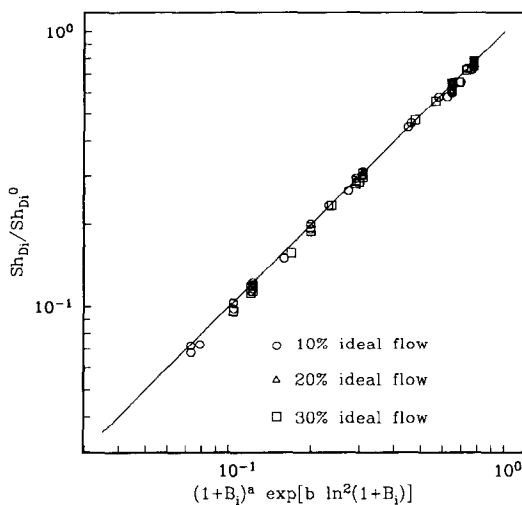


FIG. 7. Effect of tangential surface velocity on Sherwood number.

Renksizbulut and Haywood [2], the maximum surface velocity may be as large as 24% of the free stream velocity (that is, $\delta \sim 0.16$). Over 800 calculations have been carried out assuming 10, 20 or 30% ($\delta = 0.1, 0.2$ and 0.3 , respectively) of the ideal flow velocity at the sphere surface for mono and bicomponent liquid spheres. The results were used to perform a sensibility analysis of the correlated ratios Nu_D/Nu_D^0 and $Sh_{D_1}/Sh_{D_1}^0$, where the dimensionless numbers without phase change are those obtained for the same surface velocity condition. The comparison between these data points and the correlations obtained for the ratios of Nusselt and Sherwood numbers, equations (37) and (38), are shown in Figs. 6 and 7, respectively. For the case of 10% ideal flow velocity, the largest deviation for the Nusselt number ratio is 26% and for

the Sherwood ratio is 8%. For the largest assumed surface velocity, these maximum errors are 30% and 8%, respectively. For all cases, the mean deviation between calculated ratios and the correlations is less than 4.5%. Since these deviations are in the range of accuracy of the correlations and of the Nusselt and Sherwood numbers, the effect of surface velocity is completely taken in account through the variation of Nu_D^0 and $Sh_{D_1}^0$. Thus, the correlations obtained above are still valid for a surface tangential velocity different from zero.

CONCLUSIONS

The solution of constant-property boundary-layer equations for momentum, mass and energy transport in the flow over a sphere and their coupled boundary conditions is obtained by series solution. The interdiffusion term in the energy equation is considered in the analysis. Only the first three terms in the series are retained and it has been verified that, for most cases, they suffice to determine the heat and mass transfer characteristics of the flow.

The results of a large number of calculations are presented in the form of ratios of Nusselt and Sherwood numbers with and without phase change. These calculations span a large range of the relevant dimensionless parameters. The data points have been correlated by the heat and mass transfer numbers, defined in terms of the mean specific heat for the flow and the fraction rates of phase change. A global interdiffusion parameter is defined and it is shown that the Nusselt number ratio is better correlated when this parameter is included. Due to the large range of transfer numbers considered, a power dependency on the transfer numbers is not enough to represent the data. High order correlations are presented which better represent the data trends. The obtained blowing corrections represent the high Reynolds number asymptotes to be used in the extended film theory. The resulting correlations for the Nusselt and Sherwood numbers are then applicable for $0 \leq Re_D \leq 1000$.

The validity of the determined correlations when the surface tangential velocity is different from zero is evaluated through sensibility analysis. The surface tangential velocity is assumed to be equal to a fraction (10, 20 and 30%) of the ideal flow tangential velocity and the Nusselt and Sherwood numbers are then evaluated for several cases in the studied range of parameters. Correlations for the Nusselt number for cases with no phase change are determined and the ratios of Nusselt and Sherwood numbers with and without phase change are then compared with the correlations derived previously for no surface velocity. The good agreement between correlations and data points allows one to extend the validity of the obtained blowing corrections for a general surface velocity condition.

Acknowledgements—One of the authors (P. L. C. Lage)

would like to acknowledge the financial support from CNPq, Grant No. 202129/90.0. This research was supported in part by the University of California, Irvine, through an allocation of computer time. The computations were performed on the Cray Y-MP at the San Diego Supercomputing Center.

REFERENCES

1. G. L. Hubbard, V. E. Denny and A. F. Mills, Droplet vaporization effects of transients and variable properties, *Int. J. Heat Mass Transfer* **18**, 1003–1008 (1975).
2. M. Renssizbulut and R. J. Haywood, Transient droplet evaporation with variable properties and internal circulation at intermediate Reynolds numbers, *Int. J. Multiphase Flow* **14**, 189–202 (1988).
3. R. J. Haywood, R. Nafziger and M. Renssizbulut, A detailed examination of gas and liquid phase transient processes in convective droplet evaporation, *J. Heat Transfer* **111**, 495–502 (1989).
4. M. Renssizbulut, R. Nafziger and X. Li, A mass transfer correlation for droplet evaporation in high-temperature flows, *Chem. Engng Sci.* **46**(9), 2351–2358 (1991).
5. M. Bussmann and M. Renssizbulut, Convective evaporation of an extremely volatile fuel droplet, *J. Thermophys. Heat Transfer* **4**(4), 527–529 (1990).
6. W. E. Ranz and W. R. Marshall, Evaporation from drops, *Chem. Engng Prog.* **48**, 141–146 and 173–180 (1952).
7. M. Renssizbulut and M. C. Yuen, Experimental study of droplet evaporation in a high-temperature air stream, *J. Heat Transfer* **105**, 384–388 (1983).
8. M. Renssizbulut and M. C. Yuen, Numerical study of droplet evaporation in a high-temperature stream, *J. Heat Transfer* **105**, 389–397 (1983).
9. B. Abramzon and W. A. Sirignano, Approximate theory of a single droplet vaporization in a convective field: effects of variable properties, Stefan flow and transient liquid heating, *Proc. 2nd ASME–JSME Thermal Engng Joint Conf.*, Honolulu, Hawaii, Vol. 1, pp. 11–18 (1987).
10. B. Abramzon and W. A. Sirignano, Droplet vaporization model for spray combustion calculations, *Int. J. Heat Mass Transfer* **32**, 1605–1618 (1989).
11. R. B. Bird, W. E. Stewart and E. N. Lightfoot, *Transport Phenomena*. Wiley, New York (1960).
12. C. G. Downing, The effect of mass transfer on heat transfer in the evaporation of drops of pure liquids, Ph.D. Thesis, University of Wisconsin, Madison (1960).
13. M. Renssizbulut, Energetics and dynamics of droplet evaporation in high temperature intermediate Reynolds number flows, Ph.D. Thesis, Northwestern University, Evanston (1981).
14. S. Prakash and W. A. Sirignano, Theory of convective droplet vaporization with unsteady heat transfer in the circulating liquid phase, *Int. J. Heat Mass Transfer* **23**, 253–268 (1980).
15. V. Pereyra, PASVA3: an adaptive finite-difference FORTRAN program for first order non-linear boundary value problems, *Lectures Notes in Computer Science* **76**, 67–68 (1978).